Development of poly(ethylene glycol) diacrylate membrane for facilitated CO_2/N_2 separation

T P Kim[1], Z A Jawad[2] and B L F Chin[1]

[1] Department of Chemical Engineering, Faculty of Engineering and Science, Curtin University Malaysia, CDT 250, 98009 Miri, Sarawak, Malaysia

[2] Department of Chemical Engineering, College of Engineering, Qatar University, P.O.Box: 2713, Doha, Qatar

Email: zjawad@qu.edu.qa

Abstract. Carbon dioxide (CO_2) is responsible for approximately 80% of greenhouse gases emission that is the main source to global climate change causing notable environmental impacts. Poly (ethylene glycol) diacrylate (PEGDA) have polar PEG repeating units, which provide a strong affinity towards carbon dioxide (CO_2) molecules has been blended with 3-aminopropyltrimethoxysilane (APTMS) to synthesize membrane for CO_2 /nitrogen (N_2) separation. The new synthesized membrane is studied for potential applications in gas separation and to be implemented in control CO_2 emission. APTMS is also used to delay the diffusion between polymer and solvent. In this study, concentration of polymer of PEGDA and casting solvent of APTMS in terms of mol ratio from a range of 0.9:1.1 to 1.3:0.7 is discussed. Based on the results, PEGDA membrane shows best gas separation performance at mol ratio of PEGDA to APTMS of 1:1 where the permeance for both CO_2/N_2, and CO_2/N_2 selectivity are 75.21±0.15 GPU, 22.95±0.05 GPU and 3.28±0.12, respectively. An optimal aminosilane/polymer reaction ratio benefits the gas separation performance of the membrane due to the affinity of the membrane towards CO_2 and formation of different membrane surface morphology.

Keywords: Membrane Technology; poly (ethylene glycol) diacrylate; 3-aminopropyltrimethoxysilane; CO_2/N_2 Separation

1. Introduction

Global climate change has been an arising issue in the recent decade prompting organizations such as Intergovernmental Panel on Climate Change into taking proper course of resolving the issue or mitigating the effects of climate change [1]. CO_2 as the primary anthropogenic GHGs emanated from power plants and industrial processes, requires proper constraint or mitigation method to control its emission. Identifying the potential of CCS, this method is executed as a major strategy to resolve the issue [2]. Among three main approaches of CCS, post-combustion capture is favourably practiced given its cost-effective and compatibility for retrofitting applications compared to oxy-fuel combustion and pre-combustion capture [3]. In comparison between conventional CO_2 separation technologies, membrane separation remains favourable in industrial application [4] because of its simple modular design allows process arrangement for retrofitting purposes in industrial and cost optimization in future applications. Membrane technology also requires less maintenance; thus, proving it a cost-effective and energy-efficient technology [5]. However, the energy requirement for this technology depends on the flue gases' partial pressure while the performance of membrane is dependent on multiple parameters such as polymer concentration and casting solution concentration [6].

The principle characteristic of membranes in gas separation applications is to control the permeation of different species limited by their performance, known as Robeson limit (permeability must be sacrificed for selectivity and vice versa) [7]. It is always challenging to have a reproducible and up-scalable method to fulfill the needs. Recently, novel and straightforward strategies have been developed to fabricate high-performance membranes [8–11].

PEGDA polymer have the potential of good mechanical and diffusive properties to be fabricated as gas separation membrane [12]. Increasing PEGDA content in the fabrication of membrane had increased the permeability of CO_2 compared to N_2 due to the strong affinity existing between polar EG repeating units and CO_2 molecules [13]. The enhancement in the mechanical properties of this membrane had significantly increased the CO_2/N_2 selectivity due to the increase in cross-linking density that reduces the pore formation and affects gas separation performance [14].

APTMS are used as crosslinking agents for membrane curing where the synthesized membrane displayed higher crosslinking density, anti-swelling ability and excellent combination between the separation layer and support layer [15]. The increase in APTMS concentration during membrane synthesis had been reduced the formation of macrovoids in the phase inversion process by delaying the mutual diffusion of polymer and solvent [16]. More resistant towards pore formation; thus, smaller pore size of membrane, and higher permeability of CO_2 compared to N_2 based on their respective activation energy required [17].

Therefore, the main aim of this research is to fabricate PEGDA membrane for CO_2/N_2 separation using different polymer and solution concentration to optimize membrane's performance. Up to date, many works have been conducted to identify the effects of polymer concentration of various polymers on the gas separation performance. However, no research on the effects of APTMS concentration has been conducted. Therefore, this research is conduct to understand the relationship between the effects of both polymer (PEGDA) and solvent (APTMS) concentration on the structure and properties of membrane. Besides that, the suitability of APTMS as a casting solvent is to be identified through this experimental work by comparing its advantages and disadvantages exhibited by the membrane synthesized.

2. Materials and Experimental Methodology

2.1. Materials

PEGDA (Purity > 97 %) and APTMS (Purity > 97 %) were obtained from Sigma-Aldrich, Malaysia, for membrane fabrication. Chloroform and acetone, ACS reagent > 99.99 %, were purchased from Merck Chemical, Malaysia.

2.2. Fabrication of PEGDA Membrane

Membranes were synthesized by dry-phase inversion. The casting solution of PEGDA membranes were prepared by mixing a mole ratio of 2 of PEGDA and APTMS in 50 wt % chloroform solution for 24 hours at 25 °C. The casting solution was then casted onto a glass plate at a thickness of 150 μm and allowed to evaporate slowly at 25 °C for 2 days in ambient temperature. Next, the neat membrane was placed in a vacuum oven at 40 °C for 24 hours as the final drying stage. Finally, the resulting membrane was peeled off the glass plate and kept in a desiccator for experiment and performance testing [18]. The concentrations of PEGDA and APTMS are tabulated in Table 1.

Table 1. Mole ratios of PEGDA and APTSM.

Membrane	PEGDA mole ratio	APTMS mole ratio
M1	0.9	1.1
M2	1.0	1.0
M3	1.1	0.9
M4	1.2	0.8
M5	1.3	0.7

2.3. Gas Separation Performance Test

To study the gas separation performance, a gas permeation tests was conducted based on the previous published work [19]. Both flow rates of the permeate and retentate streams in and out of the permeation cell were measured using the bubble gas flow meters during the gas permeation test. Three samples for each fabricated membrane were collected and tested. In this work, standard error of the readings were reported to ensure reproducibility of the data.

2.4. Characterization of Membrane Synthesized

2.4.1. Scanning Electron Microscopy (SEM). Hitachi S3500N scanning electron microscope with a Schottky type thermal field emitter (SU-70 model) was used to scan the microstructure of the membranes surfaces. The analysis was carried out in vacuum conditions ($1x10^{-8}$ Pa) at an accelerating voltage of 15 kV and a secondary electron reception angle of 30.4°. The membrane samples were coated with a layer of gold approx. 2 nm thick using BAL-TEC SCD 050 Sputter Coater from Quorum Technologies to increase conductivity and prevent charge build-up [20]. Analyses of the membranes' surface morphology were carried out at different zooming rate and higher resolution electrographs to obtain clear images. Three samples were carried out for the SEM characterization to ensure reproducibility of the experimental data.

2.4.2. Attenuated Total Reflection- Fourier Transform Infrared Spectroscopy (ATR-FTIR). A schematic of multiple reflections of internal reflection element (IRE) are illustrated in Figure 1 [21, 22]. The spectra of the membranes were recorded by a Thermo Scientific FTIR model (NICOLET iS10, USA) using diamond crystal over the wavenumber range of 4000─400 cm^{-1} with 32 scans.

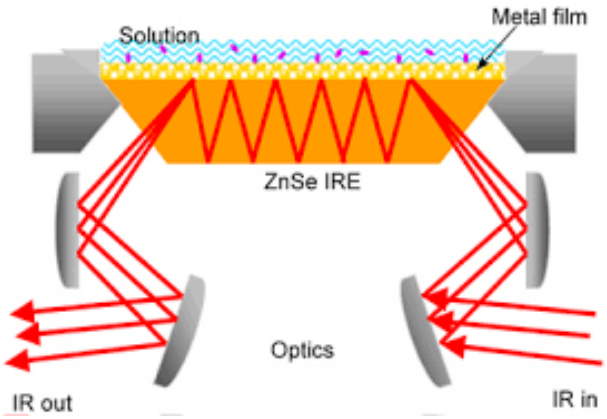

Figure 1. Schematic diagram of ATR-FTIR (I =incident radiation ; R = reflected radiation) [22].

3. Results and Discussion

3.1. The Effects of PEGDA and APTMS Concentration

The main aim of this study is to investigate the effect of the concentration of PEGDA and APTMS on the membrane structure and gas separation performance of PEGDA membrane. According to Ghadimi *et al.* (2014), the increase in the PEGDA content allows higher permeance of CO_2 through the PEGDA membrane, attributed to the dipolar-quadrupolar interactions induced by the strong affinity between the polar ethylene glycol repeating units on the membrane's structure and CO_2 molecules. The chemical affinity increases the gas permeance of CO_2 through the membrane dramatically compared to N_2 gases thus the membrane presents with a relatively high CO_2/N_2 selectivity [23].

According to Ko *et al.* (2011), the increment in the concentration of APTMS increases the affinity of the membrane towards CO_2 which confirmed through the reaction between CO_2 and primary amine, APTMS to form carbamate through a two-step zwitterion mechanism and then regeneration via zwitterion to produce APTMS, as illustrated in Figure 2 [24]. In addition, based on Ilyas *et al.* (2018),

the methoxy groups of APTMS has high affinity for CO_2 to provide sites of interaction for CO_2 solvation; thus, improving CO_2 gas permeance [25].

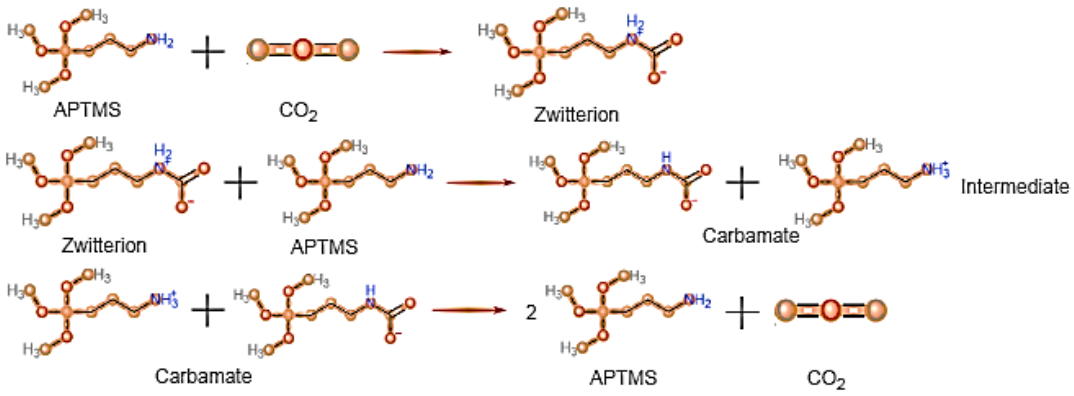

Figure 2. The expected mechanism reaction between CO_2 and primary amines [24].

3.2. ATR-FTIR Analysis

ATR-FTIR analysis was conducted to confirm the presence of organic functional groups in the PEGDA membrane fabricated with different concentration of PEGDA and APTMS of 0.9:1.1 (M1), 1.0:1.0 (M2), 1.1:0.9 (M3), 1.2:0.8 (M4) and 1.3:0.7 (M5) at a casting thickness of 150 µm. As illustrated in Figure 3, the carbonyl group of the carboxylic acid (C=O) functional group is represented by the strong absorption peaks measured at 1713.97 cm^{-1} while the peaks at 1190 cm^{-1} which justified the presence of acrylic bond (C-O) attributed to the stretching of acrylate groups [26]. Both functional groups (C=O and C-O) are ester groups. Interestingly, the disappearance of characteristic peaks of twisting vibration of the acrylic bond (CH_2=CH_2) and the deformation of CH_2=CH bond (i.e., particularly the peaks at 812 cm^{-1} and 1410 cm^{-1}) as presented in the spectra practically indicated the complete reaction conversion between PEGDA and APTMS for membranes [26].

M2 depicted the highest absorbance in relative to the absorption peaks of the PEGDA membrane compared to M1, M3, M4 and M5, as presented in table 2. The decrease in absorbance from M2 to M1 is due to the low mechanical stability of APTMS as polymer concentration of APTMS increases. This causes a lower absorption in IR radiation; thus, a lower absorption peak has been demonstrated in figure 3. Additionally, the reduction in the absorbance peaks from M2 to M5 have been explained by the SEM analysis conducted where the wrinkle formation showed in M3, M4 and M5 resulted lower absorption peaks, and reflection of the evanescent wave [27].

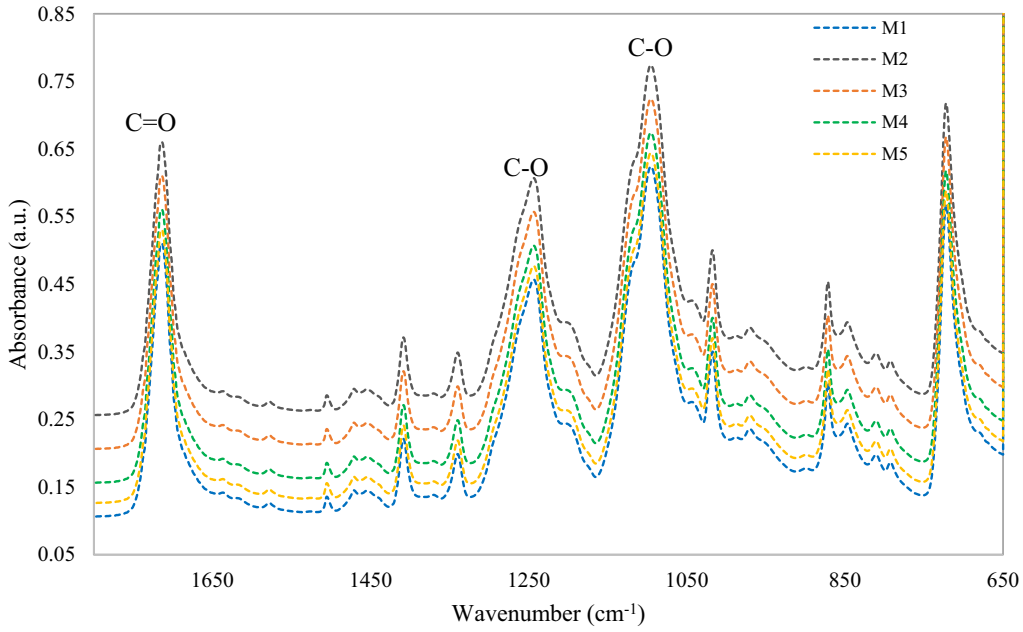

Figure 3. ATR-FTIR spectra of of membrane with different concentration of PEGDA:APTMS for M1 (0.9:1.1); M2 (1:1); M3 (1.1:0.9); M4 (1.2:0.8); M5 (1.3:0.7) at a casting thickness of 150 µm.

Table 2. Assignment of the characteristic FTIR bands of PEGDA membrane.

Vibration Stretching	Wavenumber (cm^{-1})	Absorbance				
		M1	M2	M3	M4	M5
C=O	1713.97	0.51	0.66	0.61	0.56	0.53
C-O	1240.0	0.22	0.37	0.32	0.27	0.24
C-O	1095.9	0.62	0.77	0.72	0.67	0.64

3.3. SEM Analysis

SEM is used for characterization of the physical structure and morphology of the PEGDA membrane fabricated at different concentration of PEGDA and APTMS of M1 (0.9:1.1), M2 (1.0:1.0), M3 (1.1:0.9), M4 (1.2:0.8) and M5 (1.3:0.7) at a casting thickness of 150 µm.

M1 shows a rough surface layer with formation of small molecular size defects, as observed in Figure 4a. Higher concentration of APTMS than PEGDA in M1 exhibits low mechanical stability where the evaporation of solvent forms the molecular size defects at the membrane's surface as the structural integrity of the membrane surface is weaken [28].

The SEM analysis of M2 (Figure 4b) shows a smooth surface layer. The polymer support provided by the concentration of PEGDA in M2 is able to prevent formation of molecular size defects on the membrane surface compared to M1. The hydrophilic properties exhibited by PEGDA is not significant to form wrinkles on the membrane surface as concentration of PEGDA of M2 is lower as compared to M3, M4 and M5 [29].

M3 presented with wrinkle formations on the membrane's top surface as observed in Figure 4c. The hydrophilic properties exhibited by PEGDA causes the diffusion of water vapour during air-drying of membrane to induce interfacial tension with the PEGDA at the membrane surface. The increase in the PEGDA concentration from M2 to M3 results in a stronger diffusion of water vapour through the membrane that caused folding of the membrane surface structure into a wrinkle formation [30]. Therefore, significant wrinkle formations are also observed on the membrane surface of both M4 and

M5 in Figure 4d and Figure 4e, respectively, as the PEGDA concentration increased from M3 to M4 to M5 [27].

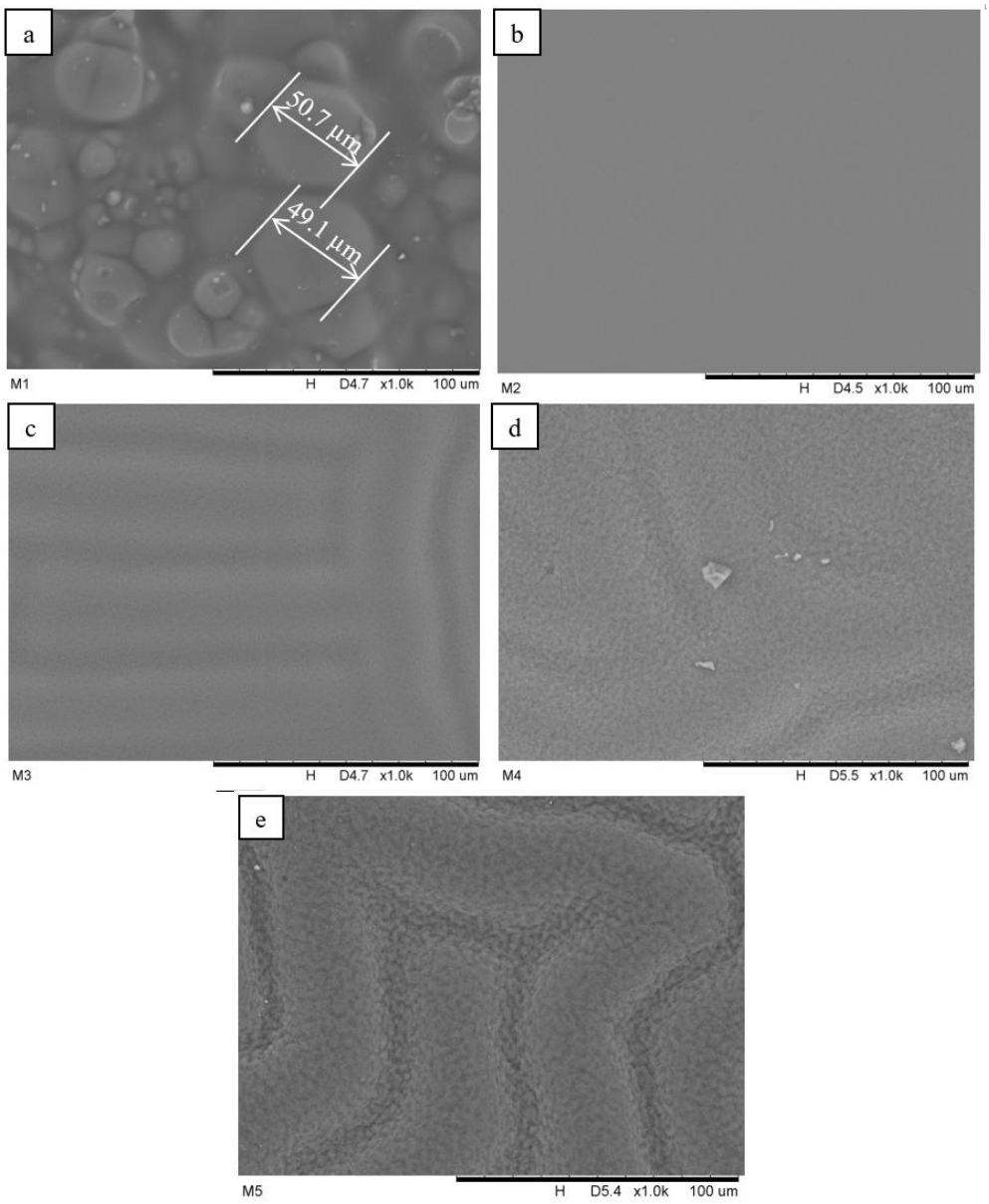

Figure 4. SEM surface morphologies of membrane with different concentration of PEGDA:APTMS for (a) M1 (0.9:1.1); (b) M2 (1:1); (c) M3 (1.1:0.9); (d) M4 (1.2:0.8); (e) M5 (1.3:0.7) at casting thickness of 150 µm.

3.4. Gas Permeation Test

Gas permeance towards CO_2 and N_2 of PEGDA membrane fabricated at different concentration of PEGDA and APTMS of M1 (0.9:1.1), M2 (1.0:1.0), M3 (1.1:0.9), M4 (1.2:0.8) and M5 (1.3:0.7) at a casting thickness of 150 µm is analysed through gas permeation test conducted using a gas permeation test rig.

3.4.1. Membrane Performance towards CO_2. As observed in Figure 5, the gas permeance of CO_2 is the highest for M2 (75.21±0.15 GPU) when the ratio of PEGDA to APTMS is 1:1 compared to M1

(69.42±0.08 GPU), M3 (72.07±0.20 GPU), M4 (70.25±0.23 GPU) and M5 (68.04±0.22 GPU). The CO_2 gas permeance had reduced from M2 to M1 as a result of the increase of APTMS concentration from M2 to M1 during the intermediate reaction between CO_2 and APTMS. Saturated adsorbed CO_2 in the form of carbamate species produced during the reaction between CO_2 and APTMS that is present in the membrane affected the gas permeance of CO_2; therefore, the gas separation performance towards CO_2 of M2 is lower than of M1 [31].

However, the decrease in CO_2 gas permeance from M2 to M5 can be interpreted as the inferior effect of the dipolar-quadrupolar interactions induced between CO_2 and PEGDA compared to the affinity exhibited by the intermediate reaction between CO_2 and APTMS to form carbamate [32]. The methoxy groups present in APTMS also verified the high affinity between CO_2 and APTMS to provide sites of CO_2 interaction; hence, increasing the gas permeance of CO_2 of the membrane as APTMS concentration increases from M5 to M2 [33]. Besides that, based on the FTIR analysis conducted, the absorption peaks recorded for C=O and C-O stretch are the highest in M2 compared to M1, M3, M4 and M5 due to the low mechanical stability in M1 and the wrinkle formations in M3, M4 and M5. Therefore, the higher absorption peaks proves the stronger dipole moment between M2 and CO_2 which is attributed to the increase in gas permeance.

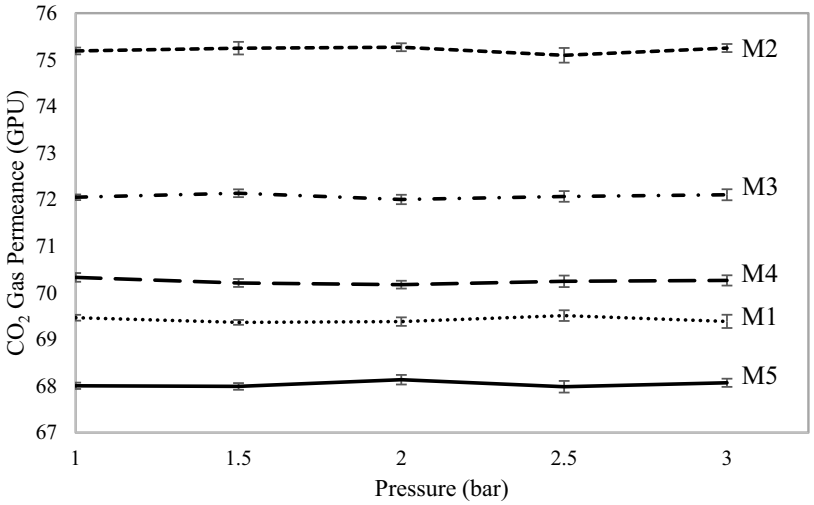

Figure 5. CO_2 permeance of membrane with different concentration of PEGDA:APTMS for M1 (0.9:1.1); M2 (1:1); M3 (1.1:0.9); M4 (1.2:0.8); M5 (1.3:0.7) at a casting thickness of 150 μm.

3.4.2. Membrane Performance towards N_2. Based on Figure 6, the N_2 permeance is the lowest for M2 (22.95±0.05 GPU) when the ratio of PEGDA to APTMS is 1:1 as compared to M1 (23.47±0.11 GPU), M3 (23.36±0.210 GPU), M4 (24.19±0.21 GPU) and M5 (24.79±0.18 GPU). The increment of N_2 permeance from M2 to M1 is a result of the formation of molecular size defects of both 49.1 μm and 50.7 μm that provided sites for gas permeation thus presented with higher permeation of N_2 gases [23]. As for membrane M3, M4 and M5 have higher gas permeance compared to M1 due to their surface morphology where the wrinkles formed on the top surface provides more interlayer is involved in the N_2 gas permeation across the membrane thus increasing the N_2 gas permeance [34].

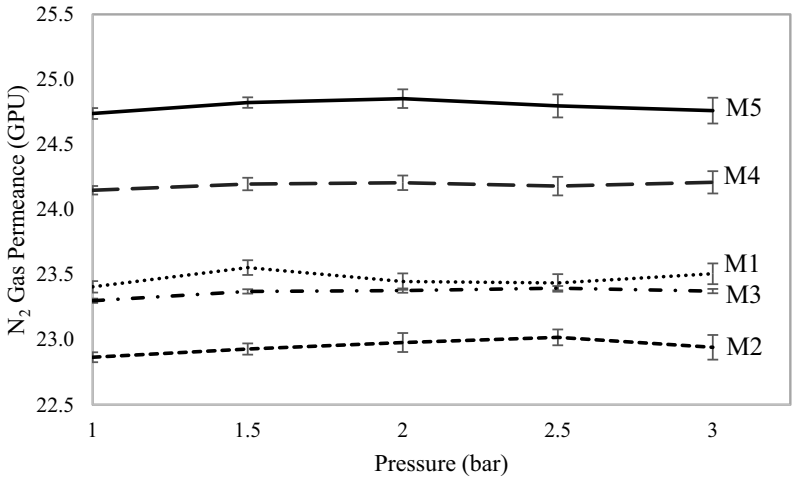

Figure 6. N_2 permeance of membrane with different concentration of PEGDA:APTMS for M1 (0.9:1.1); M2 (1:1); M3 (1.1:0.9); M4 (1.2:0.8); M5 (1.3:0.7) at a casting thickness of 150 μm.

3.4.3. Membrane Performance towards CO_2/N_2 Selectivity. According to Figure 7, the CO_2/N_2 selectivity is the highest for M2 (3.28±0.12) when the ratio of PEGDA to APTMS is 1:1 as compared to M1 (2.96±0.08), M3 (3.08±0.11), M4 (2.90±0.03) and M5 (2.74±0.13). The increasing of APTMS concentration from M2 to M1 resulted in a decrease of CO_2/N_2 selectivity from 3.28±0.12 to 2.96±0.08. This is due to the saturated carbamate species formed by the intermediate reaction between APTMS and CO_2. The saturated carbamate slows the intermediate reaction which affects the CO_2/N_2 selectivity of M1 as compared to M2 [35]. This increasing in CO_2/N_2 selectivity from M5 to M2 is attributed to the affinity between CO_2 and CO_2-affinitive moieties in APTMS (methoxy and amine groups), which is relatively stronger than the affinity between PEGDA and CO_2 as the concentration of APTMS increases from M5 to M2; thus, M5 exhibits a lower CO_2/N_2 selectivity as compared to M2 [36].

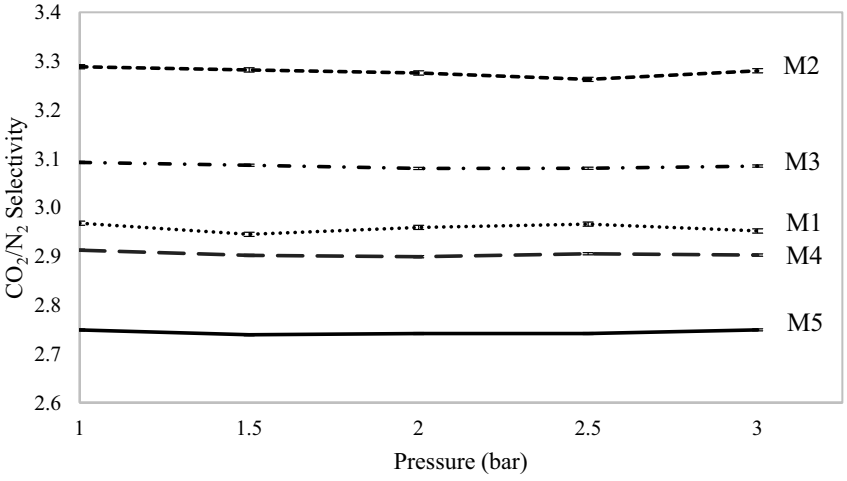

Figure 7. CO_2/N_2 selectivity of membrane with different concentration of PEGDA:APTMS for M1 (0.9:1.1); M2 (1:1); M3 (1.1:0.9); M4 (1.2:0.8); M5 (1.3:0.7) at a casting thickness of 150 μm.

In summary, M2 that has the highest CO_2 permeance (75.21±0.15 GPU) is presented with the highest CO_2/N_2 selectivity (3.278±0.12) and also the lowest N_2 gas permeance (22.95±0.05 GPU) as compared to M1, M3, M4 and M5, as illustrated in figures 5 and 6. This is due to the highest absorption peaks for both C=O and C-O stretch that represents the carbonyl group, as shown in table 2. Therefore, the higher reactivity of the membrane towards CO_2 is attributed to the high CO_2 gas permeance of M2. Besides that, the concentration of PEGDA to APTMS of M2 presents a smooth membrane surface which minimizes the gas permeance of N_2 as compared to M1 that have molecular size defects formation and M3, M4, M5 that have wrinkle formation on the membrane surface, which subsequently increases the N_2 gas permeance across the membrane [30]. The increase in APTMS concentration from M5 to M2 increases the affinity of the membrane towards CO_2 due to the higher presence of amine and methoxy group which has a stronger effect compared to the dipolar-quadrupolar interactions between PEG and CO_2. However, the increment of concentration is limited by the adsorption of CO_2 that affects the gas permeance of CO_2 [28]. Therefore, the optimized concentration of PEGDA to APTMS is determined at a mol ratio of 1:1 of M2.

Furthermore, the performance of the present work has been compared to the high performance membranes, as tabulated in table 3. It is clearly showed that the new synthesized PEGDA membrane need a further modification suggested by developing hollow fiber membrane similar to Liang *et al.* (2017) and Yong *et al.* (2013). Similarly, Naderi *et al.* (2018) proposed the addition of ethylene oxide group that could affect the overall gas permeability and selectivity because it has a high affinity towards CO_2 molecules through quadrupolar interactions [11].

Table 3. Summary of CO_2/N_2 permeation properties achieved from present work compared to previous study.

References	**Types of membrane gas separation**	***P* (CO_2)**	***P* (N_2)**	**CO_2/N_2 Ideal selectivity**
Present work	Poly (ethylene glycol) diacrylate flat sheet membrane	75.21±0.15*	22.95±0.05*	3.28
Liang *et al.* (2017)	Hollow fiber crosslinked polydimethylsiloxane membrane	3195 **	278 **	11.1
Yong *et al.* (2013)	Polymers of intrinsic microporosity /Matrimid Hollow fiber membrane	177.3*	6.7*	27.8
Naderi *et al.* (2018)	Hydrophilic polyethersulfone Flat sheet Membrane	3.74 **	0.11**	34.9

* GPU
** barrer

4. Conclusion

The main objective of this study is to synthesize effective gas separation membranes for CO_2 /N_2 gas separation. Firstly, the neat polymeric membranes PEGDA were fabricated. The performance in regards of permeance towards CO_2 and N_2, and CO_2/N_2 selectivity confirmed that the concentration of PEGDA and APTMS correlated to the membranes' structure and surface morphology as well as the Lewis acid-base interaction towards CO_2. In term of membrane separation performances, the optimal mol ratio of PEGDA and APTMS at 1:1 (M2) exhibited the highest CO_2/N_2 selectivity of (3.278±0.12) with CO_2 permeance (75.21±0.15 GPU) and N_2 permeance (22.95±0.05 GPU). Therefore, PEGDA to APTMS concentration of 1:1 mol ratio is recommended for the fabrication of PEGDA membrane to be utilized in the industrial application for CO_2/N_2 separation and efficiently reduced CO_2 emission into the atmosphere thus mitigate the effect of global warming.

References

[1] Intergovernmental Panel on Climate C 2015 Climate Change 2014: Mitigation of Climate Change: Working Group III Contribution to the IPCC Fifth Assessment Report (Cambridge: Cambridge University Press)

[2] Gale J, Abanades J, Bachu S and Jenkins C 2015 Special Issue commemorating the 10th year anniversary of the publication of the Intergovernmental Panel on Climate Change Special Report on CO_2 Capture and Storage vol 40

[3] Bui M, Adjiman C S, Bardow A, Anthony E J, Boston A, Brown S, Fennell P S, Fuss S, Galindo A and Hackett L A 2018 Carbon capture and storage (CCS): the way forward *Energy & Environ. Sci.* **11** 1062–176

[4] Kim J, Fu Q, Xie K, Scofield J M P, Kentish S E and Qiao G G 2016 CO2 separation using surface-functionalized SiO_2 nanoparticles incorporated ultra-thin film composite mixed matrix membranes for post-combustion carbon capture *J. Membr. Sci.* **515** 54–62

[5] Scofield J M P, Gurr P A, Kim J, Fu Q, Kentish S E and Qiao G G 2016 Blends of fluorinated additives with highly selective thin-film composite membranes to increase CO_2 permeability for CO_2/N_2 gas separation applications *Ind. Eng. Chem. Res.* **55** 8364–72

[6] Sani N A A, Lau W J and Ismail A F 2015 Morphologies and separation characteristics of polyphenylsulfone-based solvent resistant nanofiltration membranes: Effect of polymer concentration in casting solution and membrane pretreatment condition *Korean J. Chem. Eng.* **32** 743–52

[7] Robeson L M 2008 The upper bound revisited *J. Membr. Sci.* **320** 390–400

[8] Liang C Z, Yong W F and Chung T S 2017 High-performance composite hollow fiber membrane for flue gas and air separations *J. Membr. Sci.* **541** 367–77

[9] Yong W F, Li F Y, Xiao Y C, Chung T S and Tong Y W 2013 High performance PIM-1/Matrimid hollow fiber membranes for CO2/CH4, O2/N2 and CO2/N2 separation *J. Membr. Sci.* **443** 156–69

[10] Yong W F, Kwek K H A, Liao K S and Chung T S 2015 Suppression of aging and plasticization in highly permeable polymers *Polymer* **77** 377–86

[11] Naderi A, Yong W F, Xiao Y, Chung T S, Weber M and Maletzko C 2018 Effects of chemical structure on gas transport properties of polyethersulfone polymers *Polymer* **135** 76–84

[12] Anna C, Marta M, Ugo M, Giulia L M and Alessandro S 2017 Photo-crosslinked poly(ethylene glycol) diacrylate (PEGDA) hydrogels from low molecular weight prepolymer: Swelling and permeation studies *J. Appl. Polym. Sci.* **134** 1–9

[13] Teramoto N, Wakayama K, Harima M, Shimasaki T and Shibata M 2017 *Advances in Bioinspired and Biomedical Materials Volume 2*: American Chemical Society) pp 79–91

[14] Saimani S, Dal-Cin M M, Kumar A and Kingston D M 2010 Separation performance of asymmetric membranes based on PEGDA/PEI semi-interpenetrating polymer network in pure and binary gas mixtures of CO_2, N_2 and CH_4 *J. Membr. Sci.* **362** 353–9

[15] Wu H, Zhang X, Xu D, Li B and Jiang Z 2009 Enhancing the interfacial stability and solvent-resistant property of PDMS/PES composite membrane by introducing a bifunctional aminosilane *J. Membr. Sci.* **337** 9

[16] Hisayuki N, Keisuke I, Kensuke M, Noriyasu O and Minoru T 2011 Effect of chemical structure of silane coupling agent on interface adhesion properties of syndiotactic polypropylene/cellulose composite *J. Appl. Polym. Sci.* **119** 1732–41

[17] Madaeni S S and Taheri A H 2011 Effect of Casting Solution on Morphology and Performance of PVDF Microfiltration Membranes *Chem Eng Technol* **34** 1328–34

[18] Mazzoccoli J P 2008 Properties of Poly(ethylene glycol) Diacrylate Blends and Acoustically Focused Multilayered Biocomposites Developed for Tissue Engineering Applications. Case Western Reserve University)

[19] Jawad Z, Ahmad A, Low S and Zein S 2015 Incorporation of inorganic carbon nanotubes fillers into the CA polymeric matrix for improvement in CO_2/N_2 separation *Curr. Nanosci.* **11** 69–79

[20] Kowalik-Klimczak A, Bednarska A, Grądkowski M and Gierycz P 2016 Scanning Electron Microscopy (SEM) in the analysis of the structure of polymeric nanofiltration membranes *Problemy Eksploatacji* **100** 119–28

[21] Georg R and Bernhard L 2013 *Encyclopedia of Analytical Chemistry,* pp
[22] Andrew Chan K L and Kazarian S G 2016 Attenuated total reflection Fourier-transform infrared (ATR-FTIR) imaging of tissues and live cells *Chem. Soc. Rev.* **45** 1850–64
[23] Ghadimi A, Amirilargani M, Mohammadi T, Kasiri N and Sadatnia B 2014 Preparation of alloyed poly (ether block amide)/poly (ethylene glycol diacrylate) membranes for separation of CO2/H2 (syngas application) *J. Membr. Sci.* **458** 14–26
[24] Ko Y G, Shin S S and Choi U S 2011 Primary, secondary, and tertiary amines for CO_2 capture: Designing for mesoporous CO_2 adsorbents *J. Colloid Interface Sci.* **361** 594–602
[25] Ilyas A, Muhammad N, Gilani M A, Vankelecom I F and Khan A L 2018 Effect of zeolite surface modification with ionic liquid [APTMS][Ac] on gas separation performance of mixed matrix membranes *Sep. Purif. Technol.* **205** 176–83
[26] Lin H, Kai T, Freeman B D, Kalakkunnath S and Kalika D S 2005 The Effect of cross-linking on gas permeability in cross-linked poly(ethylene glycol diacrylate) *Macromolecules* **38** 8381–93
[27] Zhang J, Wang N, Liu W, Zhao X and Lu W 2013 Intermolecular hydrogen bonding strategy to fabricate mechanically strong hydrogels with high elasticity and fatigue resistance *Soft Matter* **9** 6331–7
[28] Ismail A F, Khulbe K C and Matsuura T 2015 *Gas Separation Membranes: Polymeric and Inorganic*: Springer International Publishing, Cham) pp 37–192
[29] Gray M L, Soong Y, Champagne K J, Pennline H, Baltrus J P, Stevens R W, Khatri R, Chuang S S C and Filburn T 2005 Improved immobilized carbon dioxide capture sorbents *Fuel Process. Technol.* **86** 1449–55
[30] Yu X, Wang Y, Li L, Li H and Shang Y 2017 Soft and wrinkled carbon membranes derived from petals for flexible supercapacitors *Sci. Rep.* **7** 45378
[31] Fu Y J, Hu C C, Lee K R and Lai J Y 2006 Separation of ethanol/water mixtures by pervaporation through zeolite-filled polysulfone membrane containing 3-aminopropyltrimethoxysilane *Desalination* **193** 119–28
[32] Liu L, Han X, Hu W, Zhao B and Fan A 2017 Desulfurization performance of polydimethylsiloxane membranes by pervaporation: Effect of crosslinking agents *Polym. Eng. Sci.* **57** 1127–35
[33] Ilyas A, Muhammad N, Gilani M A, Ayub K, Vankelecom I F J and Khan A L 2017 Supported protic ionic liquid membrane based on 3-(trimethoxysilyl)propan-1-aminium acetate for the highly selective separation of CO_2 *J. Membr. Sci.* **543** 301–9
[34] Ismail A F, Kusworo T, Mustafa A and Hasbulla H 2005 Understanding the solution-diffusion mechanism in gas separation membrane for engineering students. In: *Regional Conference on Engineering Education RCEE,*
[35] Ashjari H R, Ahmadi A and Dorraji M S S 2018 Synthesis and employment of PEGDA for fabrication of superhydrophilic PVDF/PEGDA electrospun nanofibrous membranes by in-situ visible photopolymerization *Korean J Chem Eng* **35** 289–97
[36] Panwar K, Jassal M and Agrawal A K 2015 In situ synthesis of Ag–SiO_2 Janus particles with epoxy functionality for textile applications *Particuology* **19** 107–12